2014 IEEE International Conference on Robotics & Automation (ICRA)
Hong Kong Convention and Exhibition Center
May 31 - June 7, 2014. Hong Kong, China

Symmetry Cooperative Object Transportation by Multiple Humanoid Robots

Meng-Hung Wu, Atsushi Konno, Shuhei Ogawa, Shunsuke Komizunai

***Abstract*— This research aims to create a framework of transporting an object by multiple humanoid robots. In this work, a symmetric hybrid position/force control is adapted to two humanoid robots. The reference object position and attitude are given by an operator online, and the two humanoid robots generate its whole body motion to follow the reference object position properly. The result of proposed method is verified with a dynamics simulation.**

I. INTRODUCTION

Among all types of robots, humanoid robots have the potential to handle multiple tasks and walk on uneven terrain, like human beings. Hence, it is considered that humanoid robots might be possible to work instead of humans at dangerous zones such as plant facilities.

However, there is a limitation of actuator output, so the humanoid robots are unable to perform dexterously and effectively as human beings. Although robots could be enforced by attaching more powerful motors, the output of motors is proportional to the size and weight of motors and there is a load capacity limit in robots meanwhile. Therefore, multiple humanoid robots working cooperatively will be a solution to exploit the capability of robots, and which enables robots to carry a heavy object, or bend a tough object together.

The style of cooperation of multiple robots can be classified into two types generally:

(I) *Leader-follower type*: one robot recognizes its position, makes moving plan itself or is operated directly by a human operator, which is called leader robot. Then the other robots, which are called follower robots, just follow the leader robot [1].

(II) *Symmetry type*: there is no apparent leader robot, and a central controller controls all the robot in the same time [2]. The central controller requires all information of the controlled robots.

In type (I), the force-controlled follower robots follow the position-controlled leader robot. The impedance of the follower robots has to be small to strictly follow the motion of the leader robot. Hence disturbance from environments may seriously affect on the stability of the robots. Moreover, the follower robot starts planning after the leader robot moves as illustrated in Fig. 1 (a). This time-lag may cause low responsibility and an unexpected falling down. In type (II), the reference object position is equally used for controlling the robots by a central controller. Furthermore, the two robots synchronously move and stop as illustrated in Fig. 1 (b). This synchronously movement achieves high responsibility and robustness in carrying an object.

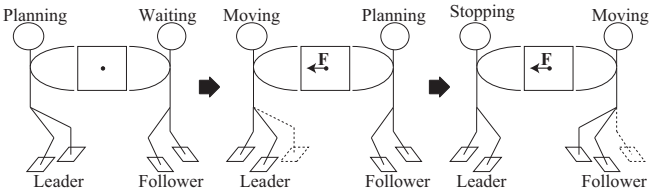

(a)Leader-follower type

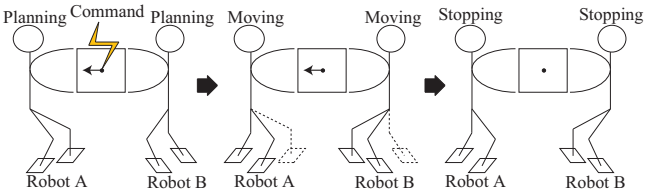

(b) Symmetry type

Fig. 1. Conceptual difference of the two types of cooperation

For those reasons, the symmetry type is studied in this research for cooperation between two humanoid robots.

Uchiyama and Dauchez proposed a central control law for controlling two robot arms without distinguishing master and slave [2]. But the redundancy of internal force is unconsidered if there are more than two arms. This control law is extended to fit controlling of four robot arms in this research. There are some ongoing researches about cooperation transportation by robots [1][3], but most of them focus on wheeled robots. However, a humanoid robot uses discrete foot placement while moving which makes it more difficult to accelerate or decelerate suddenly. Also, internal force between the robots may result in falling down because the stability margin (e.g. margin of zero moment point from the fringe of the support polygon) of a moving humanoid robot maybe not always big enough. Also there is a research studies in cooperative object transportation between a humanoid robot and a human [4]. But it turns out that the human adjusts himself to fit the humanoid robot's movement. As a result, to achieve cooperative object transportation by humanoid robots is more difficult than by wheeled robots, and has not been realized yet.

M.H. Wu, A. Konno, S. Ogawa, and S. Komizunai are with Division of System Science and Informatics, Graduate School of Information Science and Technology, Hokkaido University, Kita 14, Nishi 9, Kita-ku, Sapporo, Hokkaido, 060-0814, Japan. {wu, ogawa}@scc.ist.hokudai.ac.jp, {konno, komizunai}@ssi.ist.hokudai.ac.jp

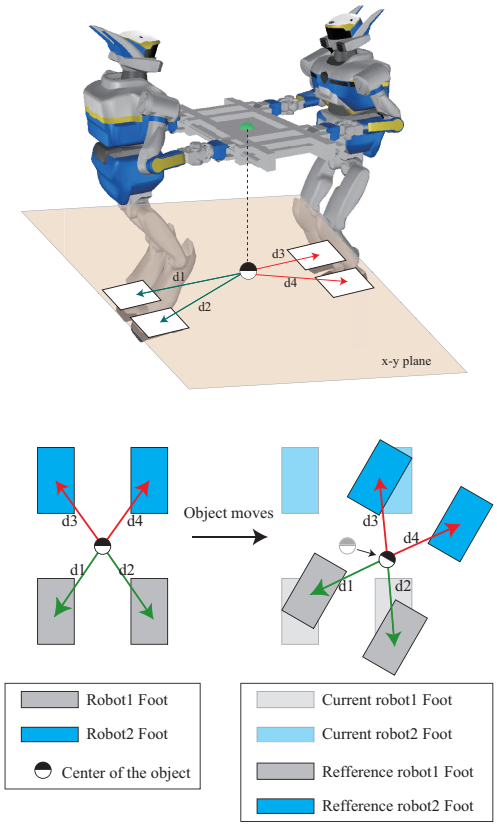

Fig. 2. Scheme of this framework

This research aims to create a framework of cooperative object transportation for humanoid robots. The scheme of the framework is shown in Fig. 2. At first, each robot records the relative displacement from the center of the grasped object to their foot position in x-y plane (d1–d4). The relative displacement is set as constant, and the reference footprint position is calculated with this constants from the object position. Next, an operator gives a reference velocity of the grasped object. The object reference position is calculated by integrating the reference velocity, and the robot arms move the object to follow the reference trajectory. The reference footprint positions are continuously calculated while the object is moving. When the error between the current and reference footprint position exceeds a specified threshold the robots start to walk. After a few walks, the robots will stop if the error is under the threshold. The center of the grasped object is always controlled by hybrid position/force control law in order to keep the previously specified internal force between the two robots while moving.

II. Workspace Vectors Describing Coordinated Tasks

In this research, the extended hybrid position/force controller is derived based on the kinematics and the statics of the four arms. In this section, the kinematic and static equations are derived using the task vectors proposed in [2], which involves generalized forces, velocities and positions.

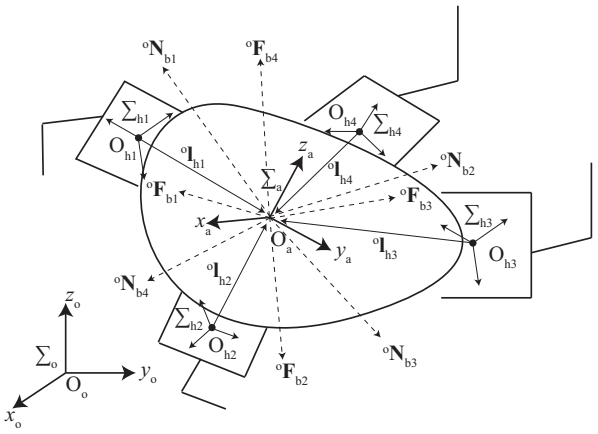

Fig. 3. A quad-arm manipulator holding a single object

Let us consider four arms holding an object as shown in Fig. 3. Σ_o, Σ_{hi} and Σ_a represent the base frame, hand frame of arm i, and the object frame, respectively. The object frame is fixed to the object. The virtual sticks ${}^o\mathbf{l}_{hi}$ $(i = 1 \sim 4)$ are determined at the moment the robots hold the object as vectors from O_i to O_a. The virtual sticks is fixed to the hand frame Σ_{hi}. Let h1 and h2 be two arms of one robot, while h3 and h4 be two arms of the other one. The deformation of the object and the slippage of the hands on object are assumed to be very small in this research, i.e. the relative position between the object center and the grasping points are constants. And in practical use, the relative position and posture information of the two robots can be computed from their joint angle information.

A. Workspace Force Vectors

The force/moment vectors ${}^o\mathbf{f}_{bi}$ at the tips of the four virtual sticks are denoted as

$$ {}^o\mathbf{f}_{bi} = \begin{bmatrix} {}^o\mathbf{F}_{bi}^T & {}^o\mathbf{N}_{bi}^T \end{bmatrix}^T , \tag{1} $$

where ${}^o\mathbf{F}_{bi} \in 3 \times 1$ is force vector, and ${}^o\mathbf{N}_{bi} \in 3 \times 1$ is moment vector. The resultant force and moment vectors ${}^o\mathbf{f}_a$ at the object are given by

$$ {}^o\mathbf{f}_a = \begin{bmatrix} {}^o\mathbf{F}_a^T & {}^o\mathbf{N}_a^T \end{bmatrix}^T = \mathbf{W}\ {}^o\mathbf{q}_b \ , $$

$$ \mathbf{W} \equiv \begin{bmatrix} \mathbf{I}_6 & \mathbf{I}_6 & \mathbf{I}_6 & \mathbf{I}_6 \end{bmatrix} \ , $$

$$ {}^o\mathbf{q}_b \equiv \begin{bmatrix} {}^o\mathbf{f}_{b1}^T & {}^o\mathbf{f}_{b2}^T & {}^o\mathbf{f}_{b3}^T & {}^o\mathbf{f}_{b4}^T \end{bmatrix}^T \ , \tag{2} $$

where $\mathbf{I}_n$ represents the $n \times n$ unit matrix. The matrix $\mathbf{W}$ maps the 24–dimensional vector ${}^o\mathbf{q}_b$ into the 6–dimensional vector ${}^o\mathbf{f}_a$. The rank of $\mathbf{W}$ is 6, therefore the null space of $\mathbf{W}$ is 18–dimension. i.e. the outer force/moment acts on the object is 6–dimension, and the internal force/moment , which is independent from the movement of the object, is 18–dimension. Since the null space is 18–dimension, we can make 18–dimensional vector space corresponding to the null space by choosing a proper vector set of 18–dimension,

which is orthogonal to each other. The vector space is chosen as:

$$\mathbf{V} = \begin{bmatrix} \mathbf{I}_6 & \mathbf{I}_6 & \mathbf{O}_6 \\ \mathbf{I}_6 & -\mathbf{I}_6 & \mathbf{O}_6 \\ -\mathbf{I}_6 & \mathbf{O}_6 & \mathbf{I}_6 \\ -\mathbf{I}_6 & \mathbf{O}_6 & -\mathbf{I}_6 \end{bmatrix}, \tag{3}$$

where $\mathbf{O}_n$ represents the $n \times n$ zero matrix. Then we define a 18–dimensional vector ${}^o\mathbf{f}_n$, which belongs to this null space, and when ${}^o\mathbf{f}_a$ is given the general solution of (2) becomes as follows:

$${}^o\mathbf{q}_b = \mathbf{W}^\dagger \, {}^o\mathbf{f}_a + \mathbf{V} \, {}^o\mathbf{f}_n \ , \tag{4}$$

where $\mathbf{W}^\dagger$ is the pseudo-inverse matrix of $\mathbf{W}$. The workspace force/moment vector ${}^o\mathbf{h}$ is defined as:

$${}^o\mathbf{h} = \begin{bmatrix} {}^o\mathbf{f}_a^T & {}^o\mathbf{f}_n^T \end{bmatrix} \ . \tag{5}$$

(4) is rewritten using ${}^o\mathbf{h}$ as follows:

$${}^o\mathbf{q}_b = \mathbf{U} \, {}^o\mathbf{h} \tag{6}$$

where $\mathbf{U} = \begin{bmatrix} \mathbf{W}^\dagger & \mathbf{V} \end{bmatrix}$. As a result, ${}^o\mathbf{h}$ could be computed when ${}^o\mathbf{q}_b$ is given as follows:

$${}^o\mathbf{h} = \mathbf{U}^{-1} \, {}^o\mathbf{q}_b \tag{7}$$

here,

$$\mathbf{U}^{-1} = \begin{bmatrix} \mathbf{I}_6 & \mathbf{I}_6 & \mathbf{I}_6 & \mathbf{I}_6 \\ \frac{1}{4}\mathbf{I}_6 & \frac{1}{4}\mathbf{I}_6 & -\frac{1}{4}\mathbf{I}_6 & -\frac{1}{4}\mathbf{I}_6 \\ \frac{1}{2}\mathbf{I}_6 & -\frac{1}{2}\mathbf{I}_6 & \mathbf{O}_6 & \mathbf{O}_6 \\ \mathbf{O}_6 & \mathbf{O}_6 & \frac{1}{2}\mathbf{I}_6 & -\frac{1}{2}\mathbf{I}_6 \end{bmatrix} \ . \tag{8}$$

The 18–dimensional vector ${}^o\mathbf{f}_n$ includes 3 sets of internal force/moment vectors and it is represented as follows:

$${}^o\mathbf{f}_n \equiv \begin{bmatrix} {}^o\mathbf{f}_r \\ {}^o\mathbf{f}_{c1} \\ {}^o\mathbf{f}_{c2} \end{bmatrix} \ . \tag{9}$$

Solution of (9) is given as follows:

$${}^o\mathbf{f}_a = {}^o\mathbf{f}_{b1} + {}^o\mathbf{f}_{b2} + {}^o\mathbf{f}_{b3} + {}^o\mathbf{f}_{b4} \ , \tag{10}$$

$${}^o\mathbf{f}_r = \frac{1}{4}{}^o\mathbf{f}_{b1} + \frac{1}{4}{}^o\mathbf{f}_{b2} - \frac{1}{4}{}^o\mathbf{f}_{b3} - \frac{1}{4}{}^o\mathbf{f}_{b4} \ , \tag{11}$$

$${}^o\mathbf{f}_{c1} = \frac{1}{2}{}^o\mathbf{f}_{b1} - \frac{1}{2}{}^o\mathbf{f}_{b2} \ , \tag{12}$$

$${}^o\mathbf{f}_{c2} = \frac{1}{2}{}^o\mathbf{f}_{b3} - \frac{1}{2}{}^o\mathbf{f}_{b4} \ . \tag{13}$$

The parameters of (11)–(13) depend on the chosen orthogonal vector sets $\mathbf{V}$. All of the vectors ${}^o\mathbf{f}_r$, ${}^o\mathbf{f}_{c1}$, and ${}^o\mathbf{f}_{c2}$ represent internal forces generated at the grasped object, and they can be controlled by giving the reference values for them. In the case of cooperation between two robots, ${}^o\mathbf{f}_r$ corresponds to the internal force generated by the two robots, while ${}^o\mathbf{f}_{c1}$ and ${}^o\mathbf{f}_{c2}$ correspond to internal forces generated between two arms of each robot.

B. Workspace Velocity and Position Vectors

If the virtual work done by ${}^o\mathbf{q}_b$ balances with the work done by ${}^o\mathbf{h}$, the absolute velocity (${}^o\mathbf{s}_a$) and the relative velocity (${}^o\Delta\mathbf{s}_r$, ${}^o\Delta\mathbf{s}_{c1}$, ${}^o\Delta\mathbf{s}_{c2}$) can be derived as:

$${}^o\mathbf{s}_a = \frac{1}{4}{}^o\mathbf{s}_{b1} + \frac{1}{4}{}^o\mathbf{s}_{b2} + \frac{1}{4}{}^o\mathbf{s}_{b3} + \frac{1}{4}{}^o\mathbf{s}_{b4} \ , \tag{14}$$

$${}^o\Delta\mathbf{s}_r = {}^o\mathbf{s}_{b1} + {}^o\mathbf{s}_{b2} - {}^o\mathbf{s}_{b3} - {}^o\mathbf{s}_{b4} \ , \tag{15}$$

$${}^o\Delta\mathbf{s}_{c1} = {}^o\mathbf{s}_{b1} - {}^o\mathbf{s}_{b2} \ , \tag{16}$$

$${}^o\Delta\mathbf{s}_{c2} = {}^o\mathbf{s}_{b3} - {}^o\mathbf{s}_{b4} \ . \tag{17}$$

According to [2], the workspace position can be derived as follows:

$${}^o\mathbf{p}_a = \frac{1}{4}{}^o\mathbf{p}_{b1} + \frac{1}{4}{}^o\mathbf{p}_{b2} + \frac{1}{4}{}^o\mathbf{p}_{b3} + \frac{1}{4}{}^o\mathbf{p}_{b4} \ , \tag{18}$$

$${}^o\Delta\mathbf{p}_r = {}^o\mathbf{p}_{b1} + {}^o\mathbf{p}_{b2} - {}^o\mathbf{p}_{b3} - {}^o\mathbf{p}_{b4} \ , \tag{19}$$

$${}^o\Delta\mathbf{p}_{c1} = {}^o\mathbf{p}_{b1} - {}^o\mathbf{p}_{b2} \ , \tag{20}$$

$${}^o\Delta\mathbf{p}_{c2} = {}^o\mathbf{p}_{b3} - {}^o\mathbf{p}_{b4} \ . \tag{21}$$

The task vectors of generalized forces, generalized velocities, generalized position are defined as

$$\mathbf{h} = \begin{bmatrix} {}^o\mathbf{f}_a & {}^a\mathbf{f}_r & {}^a\mathbf{f}_{c1} & {}^a\mathbf{f}_{c2} \end{bmatrix} \ , \tag{22}$$

$$\mathbf{u} = \begin{bmatrix} {}^o\mathbf{s}_a & {}^a\Delta\mathbf{s}_r & {}^a\Delta\mathbf{s}_{c1} & {}^a\Delta\mathbf{s}_{c2} \end{bmatrix} \ , \tag{23}$$

$$\mathbf{z} = \begin{bmatrix} {}^o\mathbf{p}_a & {}^a\Delta\mathbf{p}_r & {}^a\Delta\mathbf{p}_{c1} & {}^a\Delta\mathbf{p}_{c2} \end{bmatrix} \ , \tag{24}$$

respectively. The suffix a represents that the vector is defined with respect to the object frame $\sum_a$.

Finally, we define a Jacobian matrix $\mathbf{J}_{quad}$, which maps all joint velocities of the two robots σ to the generalized velocities is defined as:

$$\mathbf{u} = \mathbf{J}_{quad}\sigma \ . \tag{25}$$

The relationship between the joint torque Λ of the two robots and the generalized forces is given by:

$$\Lambda = \mathbf{J}_{quad}^T\mathbf{h} \ . \tag{26}$$

III. WALKING PATTERN GENERATION

A flow chart of walking planning is shown in Fig. 4. The two robots generate their own reference zero moment point (ZMP) and reference center of mass (CoM) trajectory, and hence the walking plan of two robots are independent. At first, the robots are in waiting condition. If the error between the reference footprint position and current position exceeds the previously specified threshold, the robot starts to take its first step. The error includes position error e_p and attitude error in yaw direction e_A, which are defined as:

$$e_p = \| \, \mathbf{d}^{ref} - \mathbf{d}^{cur} \, \| \ , \tag{27}$$

$$e_A = \| \, \psi^{ref} - \psi^{cur} \, \| \ , \tag{28}$$

where $\mathbf{d}^{ref}$ is the reference foot position, $\mathbf{d}^{cur}$ is the current foot position, ψ^{ref} is the reference yaw angle of the foot, and ψ^{cur} is the current yaw angle of the foot, respectively. e_p and e_A are both checked in left and right foot. After the first step,

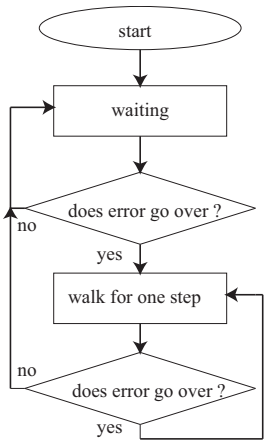

Fig. 4. Flow chart of walking planning

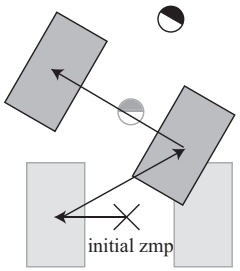

Fig. 5. The reference ZMP trajectory

the error will be checked again and the robot decides if it should stop or take a next step. Finally, the robot will stop walking when the error is under the threshold in which the arms can move the object to the desired position without stepping. The reference footprint position is calculated to meet the initial relative position from the object center to the footprint position as shown in Fig. 2. Once the reference footprint position is decided, the reference ZMP trajectory can be calculated by interpolating the discrete footprint positions (Fig. 5).

Then the reference trajectory of CoM that corresponds desired ZMP can be computed by applying the preview control of ZMP [5].

IV. CONTROL LAW OF THE WHOLE SYSTEM

The control law of the whole system consist of position control and force control.

A. Position Control–Whole Body Kinematics

Cooperation between the robots A and B is considered in this system, in which each robot has 32 degrees of freedom (DOF). The control variables in this system are: CoM position $\mathbf{p}_{CoM_{AB}}$, waist link attitude $\mathbf{R}_{waist_{AB}}$, the position and attitude of the swinging foot $\mathbf{pR}_{swingLeg_{AB}}$, the generalized object position $\mathbf{z}$, and the arm angles $\theta_{elbow_{AB}}$ (defined in [6]) of two robots, respectively. The whole system kinematics

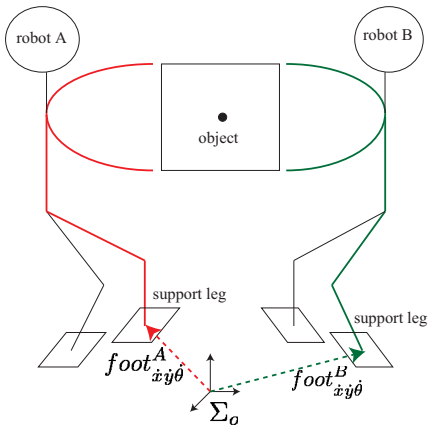

Fig. 6. The joint path for calculating J_{quad}

equation is given as follows:

$$\begin{bmatrix} \dot{\mathbf{p}}_{CoM_{AB}} \\ \dot{\mathbf{R}}_{waist_{AB}} \\ \dot{\mathbf{pR}}_{swingFoot_{AB}} \\ \dot{\mathbf{z}} \\ \dot{\theta}_{elbow_{AB}} \end{bmatrix} = \begin{bmatrix} \mathrm{diag}(\mathbf{J}_{CoM_A}, \mathbf{J}_{CoM_B}) \\ \mathrm{diag}(\mathbf{J}_{waist_A}, \mathbf{J}_{waist_B}) \\ \mathrm{diag}(\mathbf{J}_{swingFoot_A}, \mathbf{J}_{swingFoot_B}) \\ \mathbf{J}_{quad} \\ \mathrm{diag}(\mathbf{J}_{elbow_A}, \mathbf{J}_{elbow_B}) \end{bmatrix} \begin{bmatrix} \dot{\theta}^A_1 \\ \vdots \\ \dot{\theta}^A_{32} \\ \dot{\theta}^B_1 \\ \vdots \\ \dot{\theta}^B_{32} \end{bmatrix}, \tag{29}$$

where $\mathbf{J}_{CoM}$ is the CoM Jacobian matrix, $\mathbf{J}_{waist}$ is the Jacobian matrix form supporting leg to waist link, $\mathbf{J}_{swingFoot}$ is the Jacobian matrix of swing foot, $\mathbf{J}_{elbow}$ is the Jacobian matrix of arm angles, respectively. $\mathbf{z}$ and $\mathbf{J}_{quad}$ are defined in chapter II, and $\dot{\mathbf{z}}$ can be approximated by $\mathbf{u}$ (i. e. $\dot{\mathbf{z}} \approx \mathbf{u}$). The joint path for calculating $\mathbf{J}_{quad}$ is shown in Fig. 6. The $foot^i_{\dot{x}\dot{y}\dot{\theta}} (i = A, B)$ is the vector from base frame Σ_o to supporting leg, and the supporting leg switches to each other after every step. The reference trajectory of CoM and swinging foot can be calculated in the way described in chapter III. The reference attitude of the waist link is given so that the upper body maintains the upright posture, and the reference yaw angle is calculated as the mean-value of the supporting foot and swing foot. The reference object position ${}^o\mathbf{p}_a$ is given by an operator online. Since relative movement between the tips of the four virtual sticks may cause internal force, the reference ${}^o\Delta\mathbf{p}_r$, ${}^o\Delta\mathbf{p}_{c1}$, and ${}^o\Delta\mathbf{p}_{c2}$ are set to zero vectors. The reference arm angles $\theta_{elbow_{AB}}$ are set to the same arm angles in initial posture for fixing it. (29) is rewrote as:

$$\dot{\mathbf{p}}_{all} = \mathbf{J}_{all}\boldsymbol{\sigma} \ . \tag{30}$$

The whole reference joint angles of the two robots $\mathbf{q}^{ref}$ can be computed by solving inverse kinematic of (30) when reference $\mathbf{p}^{ref}_{all}$ is given. The iterative procedure is as follows:

- step1: $k = 0$, $\mathbf{q}(k) = \mathbf{q}^{cur}$.
- step2: $\mathbf{p}_{all}(k) = FK(\mathbf{q}(k))$.
- step3: if $(\mathbf{p}^{ref}_{all} - \mathbf{p}_{all}(k)) < \varepsilon$, $\mathbf{q}^{ref} = \mathbf{q}(k)$, iteration ends.
- step4: $\mathbf{q}(k+1) = \mathbf{q}(k) + \mathbf{J}^{\dagger}_{all}(\mathbf{p}^{ref}_{all} - \mathbf{p}_{all}(k))$
- step5: $k = k+1$, go to step2.

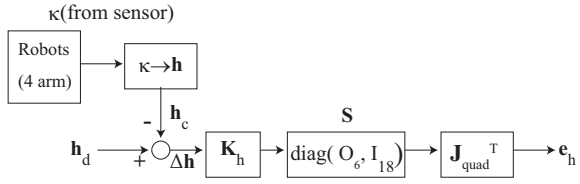

Fig. 7. Scheme of force control

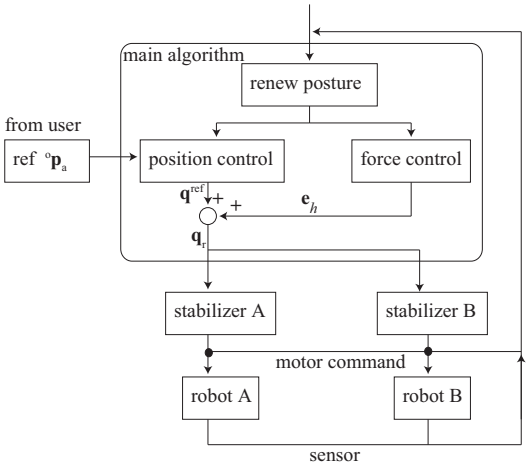

Fig. 8. Conclusion of the control law

Where $\mathbf{q}^{cur}$ is the current joint angles of the robots, FK is forward kinematics operation, ε is a specified threshold, $\mathbf{J}^{\dagger}_{all}$ is the pseudo-inverse matrix of $\mathbf{J}_{all}$, $\mathbf{q}^{ref}$ is the reference joint angles of the robots, respectively.

B. Force Control

The scheme of force control is shown in Fig. 7. $\mathbf{h}_d$ and $\mathbf{h}_c$ are desired generalized force and current generalized force, respectively. κ is the value measured by force sensor on robot's arms. $\mathbf{K}_h$ is a proper gain to transfer torque difference to angular difference. $\mathbf{S}$ is a selection matrix for internal force control. The output of force control is computed as:

$$\mathbf{e}_h = \mathbf{K}_h \mathbf{J}^T_{quad} \mathbf{S} \Delta \mathbf{h} \ . \tag{31}$$

In order to prevent the influence of robot balance, the available joints in $\mathbf{J}_{quad}$ are limited to arm joints. The control law of the whole system is concluded in Fig. 8. The reference joint angles $\mathbf{q}_r$ of the robots is computed as:

$$\mathbf{q}_r = \mathbf{q}^{ref} + \mathbf{e}_h \ . \tag{32}$$

Here, stabilizer is the balance controller.

V. DYNAMIC SIMULATION RESULT

The cooperative object transportation is simulated with the proposed method, and the system is implemented on the model of HRP-2 [7]. The proposed method is verified with dynamic simulator OpenHRP [8].

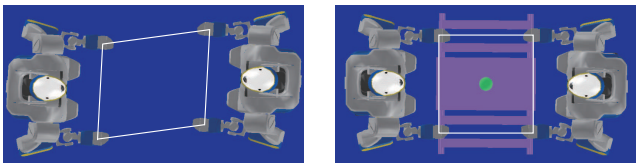

(a)Without force control (b)With force control

Fig. 9. The moving error comparison

A. The proposed Pattern Generation Method of the Whole System

First, the proposed pattern generation method verified without holding any object. The threshold of pattern generation is set as:

$$p_\varepsilon = 0.03 \ [m] \tag{33}$$

$$A_\varepsilon = 15 \ [^\circ] \tag{34}$$

where p_ε and A_ε are threshold of e_p and e_A, respectively. Fig. 9 (a) is the result after a rotation walking with 90 [°]. A relative moving of the two robots is observed in this picture. The error may be caused by the slippage between the foot and the ground, and the error will be accumulated if there is no proper force control.

B. The Effect of Force Control

Fig. 9 (b) is the result with the same operation in Fig. 9 (a) but with force control. As shown in the picture, the relative moving is eased with force control. In order to check the effect of easing internal force of the system, another simulation is done. The reference object velocity in which simulation is set as: 0.05 [m/s] in x direction,and 6 [°/s] in yaw direction. The reference velocity is kept as constant in this simulation. Fig. 10 shows the internal force ${}^o\mathbf{f}_r$ of the system in 6-axis. When the internal force is not controlled, spikes of the huge internal force are observed especially in x direction (Fig. 10 (a)). Here, x direction is the sagittal direction, and y direction is the lateral direction, respectively.

C. Walking with Online Operation

Fig. 11 shows the result of online operation. First, the reference velocity of the object (the green ball in the picture) is given as 0.05 [m/s] in x direction, and 6 [°/s] in yaw direction. After a 90 [°] rotation, the reference velocity is set to −0.05 [m/s] in x direction and 4 [m/s] in y direction. Finally, the reference velocity is set to −0.05 [m/s] in x direction, and set to zero in all direction after a few walk. Fig. 12 shows the trajectory of reference ZMP (rZMP), ZMP, CoM, and the object.

VI. CONCLUSIONS

In this paper, a framework of symmetry cooperative object transportation by two humanoid robots, which includes position-force hybrid control. Future works include consideration of the influence of the object's weight, changing the walking trajectory during one step, and verifying the proposed method with real humanoid robots.

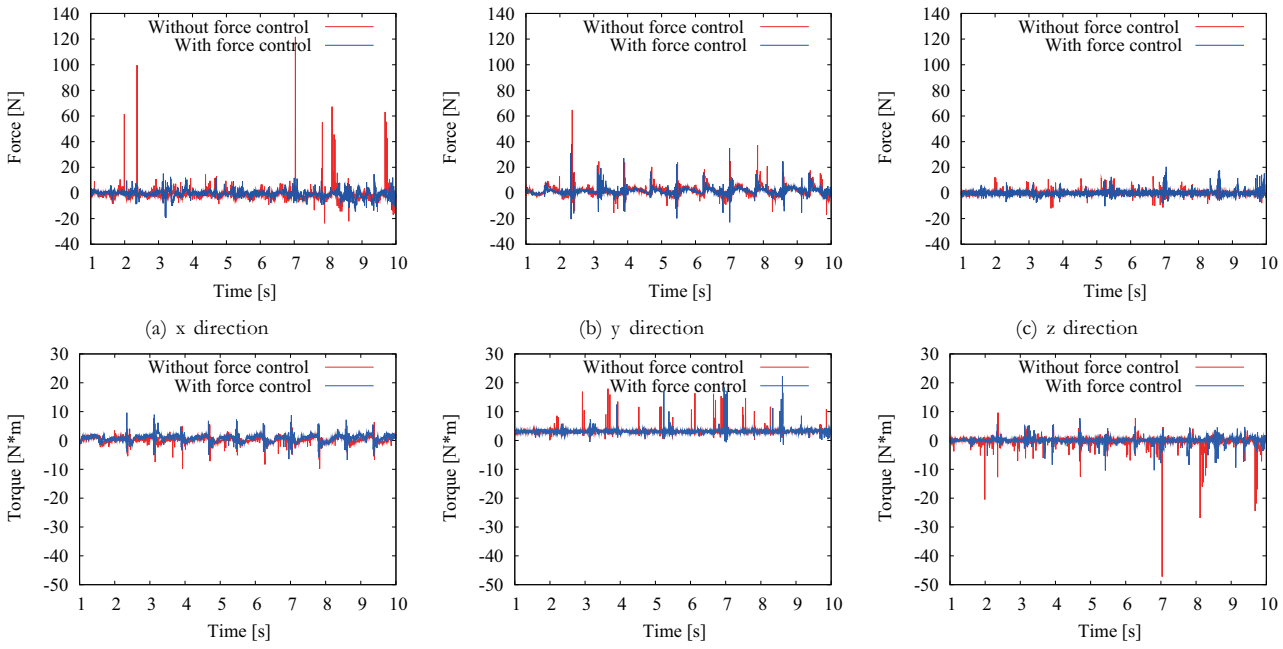

(a) x direction (b) y direction (c) z direction

(d) roll direction (e) pitch direction (f) yaw direction

Fig. 10. Internal force of six axis

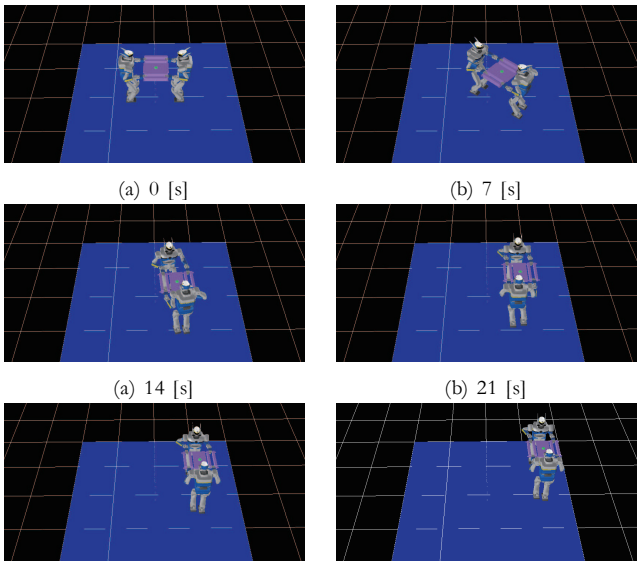

(a) 0 [s] (b) 7 [s]

(a) 14 [s] (b) 21 [s]

(a) 28 [s] (b) 35 [s]

Fig. 11. The motion of online operation

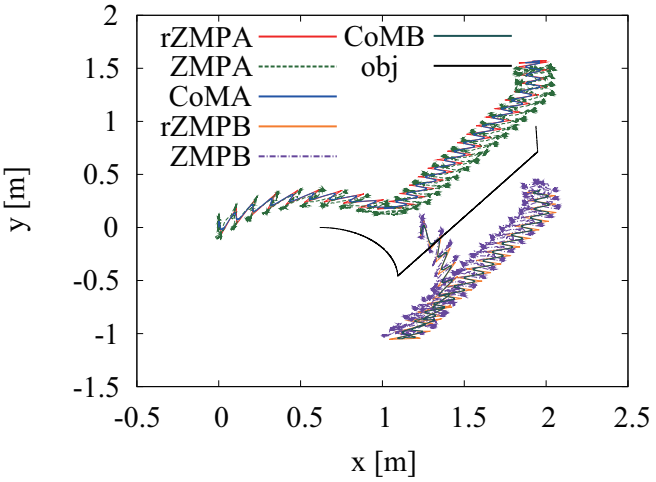

Fig. 12. Result of online operation

REFERENCES

[1] Y. Hirata, T. Sawada, Z. Wang and K. Kosuge, "Leader-Follwer Type Motion Control Algorithm of Multiple Mobile Robots with Dual Manipulators for Hanling a Single Object in Coordination," in *Int. Conf. on Intelligent Robots and Systems*, pp. 362–367, 2004.

[2] M. Uchiyama, and Dauchez, "A Symmetric hybrid position/force control scheme for the coordination of two robots," in *IEEE Int. Conf. on Robotics and Automation*, pp. 350–356, 1988.

[3] K. Kosuge, and T. Oosumi, "Decentralized Control of Multiple Robots Handling an Object,"in *IEEE Int. Conf. on Intelligent Robots and Systems*, pp. 318–323, 1996.

[4] K. Yokoyama, H. Handa, T. Isozumi, Y. Fukase, K. Kaneko, F. Kanehiro, Y. Kawai, F. Tomita, and H. Hirukawa, "Cooperative Works by a Human and a Humanoid Robot," in *IEEE Int. Conf. on Robotics and Automation*, pp. 2985–2991, 2003.

[5] S. Kajita, F. Kanehiro, K. Kaneko, K. Fujiwara, K. Harada, K. Yokoi and H. Hirukawa, "Biped Walking pattern Generation by Using Preview Control of Zero-moment Point," in *IEEE Int. Conf. on Robotics and Automation*, pp. 1620–1626, 2003.

[6] K. Kreutz-Delgado, M. Long, and H. Seraji, "Kinematic analysis of 7-dof manipulators," *International Journal of Robotics Research*, vol. 1, no. 5, pp. 469–481, 1992.

[7] K. Kaneko, F. Kanehiro, S. Kajita, H. Hirukawa, T. Kawasaki, M. Hirata, K. Akachi and T. Isozumi, "Humanoid robot HRP-2," in *IEEE Int. Conf. on Robotics and Automation*, pp. 1083–1090, New Orleans, LA, USA, 2004.

[8] F. Kanehiro, H.Hirukawa, and S.Kajita, "OpenHRP: Open Architecture Humanoid Robotics Platform," *International Journal of Robotics Research*, vol. 23, no. 2, pp. 155–165, 2004.